Bioorganic & Medicinal Chemistry xxx (2015) xxx–xxx

Contents lists available at ScienceDirect

Bioorganic & Medicinal Chemistry

journal homepage: www.elsevier.com/locate/bmc

Synthesis, structure–activity relationship and biological evaluation of novel arylpiperzines as $\alpha_{1A/1D}$-AR subselective antagonists for BPH

Fang Xu [a,*,†], Hong Chen [b,†], Jingyi Xu [c], Xue Liang [c], Xuelan He [c], Binhao Shao [c], Xianqiang Sun [d], Bing Li [e], Xiaoliang Deng [e], Mu Yuan [c,*]

[a] Institute of Tumor Pharmacology, College of Pharmacy, Jinan University, 601 West Huangpu Blvd, Guangzhou 510632, People's Republic of China
[b] College of Chemistry and Chemical Engineering, Luoyang Normal University, Luoyang, Henan 471022, People's Republic of China
[c] Pharmaceutical Research Center, Guangzhou Medical University, 195# Dongfengxi Road, Guangzhou 510182, People's Republic of China
[d] Division of Theoretical Chemistry and Biology, School of Biotechnology, KTH Royal Institute of Technology, S-106 91 Stockholm, Sweden
[e] Experimental Medical Research Center, Guangzhou Medical University, Guangzhou 510182, People's Republic of China

ARTICLE INFO

Article history:
Received 14 September 2015
Revised 2 November 2015
Accepted 19 November 2015
Available online xxxx

Keywords:
α_1-ARs
Subtype selectivity
Arylpiperazine derivatives
Antagonic activity
Homology modeling
Structure–activity relationship

ABSTRACT

A series of novel arylpiperazine derivatives as $\alpha_{1A/1D}$-adrenergic receptors (AR) subtype selective antagonists were designed, synthesized and evaluated for their antagonistic activities towards α_1-ARs (α_{1A}, α_{1B}, and α_{1D}). Compounds **9**, **12**, **13**, **15**, **17**, **18**, **21**, **22**, **25** and **26** exerted strong antagonistic effects on α_{1A} and/or α_{1D} subtypes over α_{1B} in vitro. SAR analysis indicated that chloride at the *ortho*-phenyl position for compound **17** was beneficial for the highest $\alpha_{1A/D}$-AR sub-selectivity. Moreover, molecular docking study of compound **17** with the homology-modeled α_1-ARs (α_{1A}, α_{1B}, and α_{1D}) structures exhibited differences of key amino resides in the docking pocket which may influence the subtype selectivity. ILE 193 of α_{1A} was validated as the key residues for binding ligand. This work provides useful information for finding more new potential drugs in clinic in treating benign prostatic hyperplasia (BPH).

1. Introduction

α_1-Adrenergic receptors (α_{1A}-, α_{1B}-, and α_{1D}-ARs), which belong to the G-protein coupled receptor family, play significant roles in lower urinary tract symptoms (LUTS) associated with benign prostatic hyperplasia (BPH). These receptors are widely expressed in many human tissues and involved in numerous physiological processes. Therefore, α_1-ARs are highly attractive pharmacological targets for treatment of several pathologies.[1] α_1-AR antagonists can relax the prostatic smooth muscle and are used as first-line medical treatment for patients with LUTS associated with BPH.[2] Many efforts have been devoted to the development of α_1-AR antagonists, which resulted in discovery of first-generation antagonists against α_1-ARs, such as prazosin (**I**, Fig. 1),[3] terazosin (**II**),[4] doxazosin (**III**),[5] and alfuzosin (**IV**),[6] which are used clinically for the treatment of BPH by relaxing the smooth muscle of the prostate.[7] However, these agents also exhibit side effects, including orthostatic hypotension, dizziness, decreased blood pressure, nasal congestion, and impotence, which may be partially attributed to their inability to differentiate between α_1-AR subtypes present in the prostate and those involved in maintaining vascular tone.[8] Tamsulosin (**V**, Fig. 2), the first α_{1A}-AR 'selective' antagonist, has demonstrated 15-fold selectivity for α_{1A}-AR over α_{1B}-AR and almost no selectivity for clinical trials on BPH patients. However, tamsulosin still shows side effects.[9] Naftopidil (**VI**, Fig. 2), an arylpiperazine compound, is a specific α_{1D}-adrenergic receptor antagonist,[10,11] and is one of the most widely used α_1-adrenergic receptor antagonists in Japan for the treatment of benign prostatic hyperplasia (BPH).[12,13] Other studies[14–20] have demonstrated that compounds with an open-chain linker between arylpiperazinyl and isoindole-1,3-dione-2-yl groups (e.g., NAN-190, **VII**, Fig. 2) bind to α_1-ARs with high affinity but demonstrate poor subtype selectivity. We hypothesized that the compounds with ethylbenzyl linker instead of *n*-butyl linker, such as NAN-190, will retain binding affinity and improve selectivity among the three α_1-AR subtypes (α_{1A}, α_{1B}, and α_{1D}). In the current study, we designed and synthesized (phenylpiperazinyl)ethylbenzylphthalimides derived from isoindole-1,3-diones and evaluated their antagonistic activities in the three α_1-AR subtypes. Furthermore, the homology models of α_1-ARs were built using the crystal structure of β_2-adrenergic receptor (2RH1) as template and analized the key amino residues in each binding pocket. Molecular docking was

* Corresponding authors. Tel./fax: +86 20 85220799.
E-mail addresses: xufang@jnu.edu.cn (F. Xu), mryuanmu@aliyun.com (M. Yuan).
† Contributed equally to this work.

http://dx.doi.org/10.1016/j.bmc.2015.11.020
0968-0896/

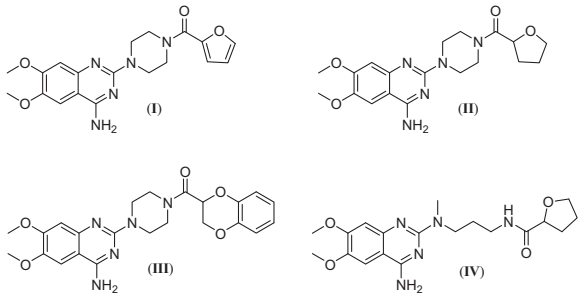

Figure 1. α_1-AR antagonists clinically used for BPH treatment. prazosin (**I**), terazosin (**II**), doxazosin (**III**), and alfuzosin (**IV**).

applied to analyze the binding mode of the representive compound with α_1-ARs and validate its subtype selectivity. The SAR was further discussed on the basis of the obtained experimental data.

2. Results and discussion

2.1. Chemistry

Arylpiperazine derivatives were designed and synthesized in order to find novel α_{1A}- and/or α_{1D}-selective ligands for the treatment of BPH, from commercially available 2-[4-(bromomethyl) phenyl]acetic acid **1** (Scheme 1). First, compound **1** was reduced to alcohol **2** in the presence of borane–methyl sulfide complex (2 M in tetrahydrofuran) at 0 °C for 1 h, then at room temperature for 10 h. The intermediate **2** was directly used without further purification. The nucleophilic substitution reaction of compound **2** with potassium phthalimide in the presence of potassium carbonate (K_2CO_3) yielded compound **3** (70% yield from compound **1**) after 16 h at reflux. Compound **3** was treated with 4-toluenesulfonyl chloride in the presence of triethylamine and a catalytic amount of 4-dimethylaminopyridine at 0 °C for 16 h to generate compound **4** (95% yield). Finally, the reactions of compound **4** with various arylpiperazines in the presence of K_2CO_3 at reflux for 16 h yielded arylpiperazine derivatives **5**–**26** (45–95% yield; Scheme 1). The structures of the compounds were confirmed by ^{1}H NMR, ^{13}C NMR, and HRMS (ESI).

2.2. Antagonistic activity in α_1-ARs

Antagonistic activities of **5**–**26** towards α_1-ARs were tested using dual-luciferase reporter assays[21] (Table 1). Compounds **9**, **12**, **13**, **15**, and **26** exhibited antagonistic effects on α_{1A} subtype (IC_{50} = 2.03, 32.43, 96.01, 89.94, 14.25 nM, respectively) and better α_{1A} subtype selectivity over α_{1B} (α_{1B}/α_{1A} ratio = 8.6–19.5). Compound **18** (IC_{50} = 35.16 nM) displayed soundly antagonistic activity on α_{1D} subtype and marked α_{1D} subtype selectivity over α_{1B} (α_{1B}/α_{1D} ratio = 22.6). Compounds **17**, **21**, **22**, and **25** also showed strong antagonistic activities both on α_{1A} (IC_{50} = 15.16, 36.14, 89.24, 46.44 nM, respectively) and α_{1D} (IC_{50} = 36.62, 16.73, 63.54, 10.07 nM, respectively), with α_{1B}/α_{1A} ratio = 4.3–51.5 and α_{1B}/α_{1D} ratio = 10.8–21.3, respectively.

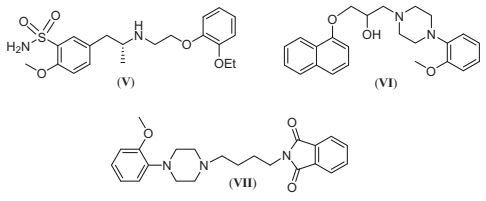

Figure 2. Structures of Tamsulosin (**V**), Naftopidil (**VI**) and NAN-190 (**VII**).

SAR analysis revealed the following results: (1) Phenylpiperazine derivative **5** exhibited better α_{1A} subtype selectivity over α_{1B} (α_{1B}/α_{1A} ratio = 5.8). However, benzylpiperazine derivative **6** showed better α_{1D} subtype selectivity over α_{1B} (α_{1B}/α_{1D} ratio = 8.7). (2) Although compounds **7**, **19**, and **24** demonstrated strong antagonistic effects on α_{1A} and α_{1D} subtypes, these compounds also exhibited strong activities in α_{1B} subtype and weak α_{1A} and/or α_{1D} subtype selectivities. (3) Compared with *o*-methyl-substituted phenyl group derivative **8** (IC_{50} = 227.70 nM and α_{1B}/α_{1A} ratio = 4.2), *p*-methyl-substituted phenyl group derivative **9** (α_{1B}/α_{1A} ratio = 14.2) exhibited strong antagonistic effects on α_{1A} subtype and better α_{1A} subtype selectivity over α_{1B}. However, compound **9** also displayed strong activity on α_{1B} subtype (IC_{50} = 28.91 nM). (4) Compounds containing an *o*-methoxyl-substituted phenyl group showed better activity on α_{1A} subtype and better α_{1A} subtype selectivity over α_{1B} than did the *p*-methoxyl substituted group, as exemplified by compounds **10** (IC_{50} = 30.12 nM and α_{1B}/α_{1A} ratio = 3.3) and **11** (IC_{50} = 884.70 nM and α_{1B}/α_{1A} ratio = 0.5). Similar result was observed in compound **13** versus **14** (IC_{50} = 229.40 nM and α_{1B}/α_{1A} ratio = 3.0). (5) Compound **12** (α_{1B}/α_{1A} ratio = 13.4) exhibited better α_{1A} subtype selectivity over α_{1B} than compound **10** (α_{1B}/α_{1A} ratio = 3.3). These results suggest that the introduction of an ethoxyl moiety at the *o*-position on the phenyl group was beneficial for improving subtype selectivity. (6) Compared with compounds **13** and **15**, compound **14** displayed decreased potency on α_{1A} subtype and lower α_{1A} subtype selectivity over α_{1B}. The obtained results suggested that a fluoro group in the *p*-position on the phenyl group was unfavorable for antagonistic activity and subtype selectivity. (7) *o*-Chloro-substituted phenyl group derivative **17** showed strong activities in α_{1A} and α_{1D} subtypes and excellent α_{1A} and α_{1D} subtypes selectivity over α_{1B}. However, *p*-chloro-substituted phenyl group derivative **18** showed strong activities in α_{1D} subtype and excellent α_{1D} subtype selectivity over α_{1B}. (8) Compounds with a cyano group at the *o*- or *p*-position or a methylsulfonyl group at the *o*-position on the phenyl group also displayed strong activities in α_{1A} and α_{1D} subtypes and better α_{1A} and α_{1D} subtypes selectivity over α_{1B}, as exemplified by compounds **21**, **22**, and **25**. (9) Compound **16** with an acetyl group at the *p*-position on the phenyl group displayed potent activity in α_{1A} subtype and excellent α_{1A} subtype selectivity over α_{1B}.

2.3. Homology model building of α_1-ARs and molecular docking studies

The structures of α_1-ARs were generated from the alignment of the template structure of β_2-AR (PDB ID 2RH1) using Schrodinger (Fig. 3). For the crystal structure of β_2-AR, the intracellular loop region 3 (IL3) was replaced by T4 lysozyme to increase the solubility and stability of the receptor, and the active site of the GPCRs was located in the extracellular region near loop 2 (EL2). IL3 loop was removed in the modeling process of the three targets since this loop was unlikely to play a major role in ligand binding. The highly conserved disulfide bond, DRY region in loop 3, NPxxY in loop 7, and CWxP in loop 6 were retained in the models. Ramachandran plot (Supplementary data in Fig. S2) of the three protein models showed that residues located in the most favored region were 90.8%, 91.7%, and 90.9%, respectively; residues located in the additionally allowed region were 7.9%, 7%, and 5.8%, respectively; residues located in the generously allowed region were 0.4%, 0.8%, and 1.7%, respectively; and residues located in the disallowed region were 0.8%, 0.4%, and 1.7%, respectively. Meanwhile, profile 3D of the three models indicated that the verified scores of the amino acid residues were more than 0.2, which was predicted to be reliable (Supplementary data in Fig. S3). The models of the three subtype proteins were considered satisfactory based on the above examples. The possible binding pockets of α_1-ARs were predicted

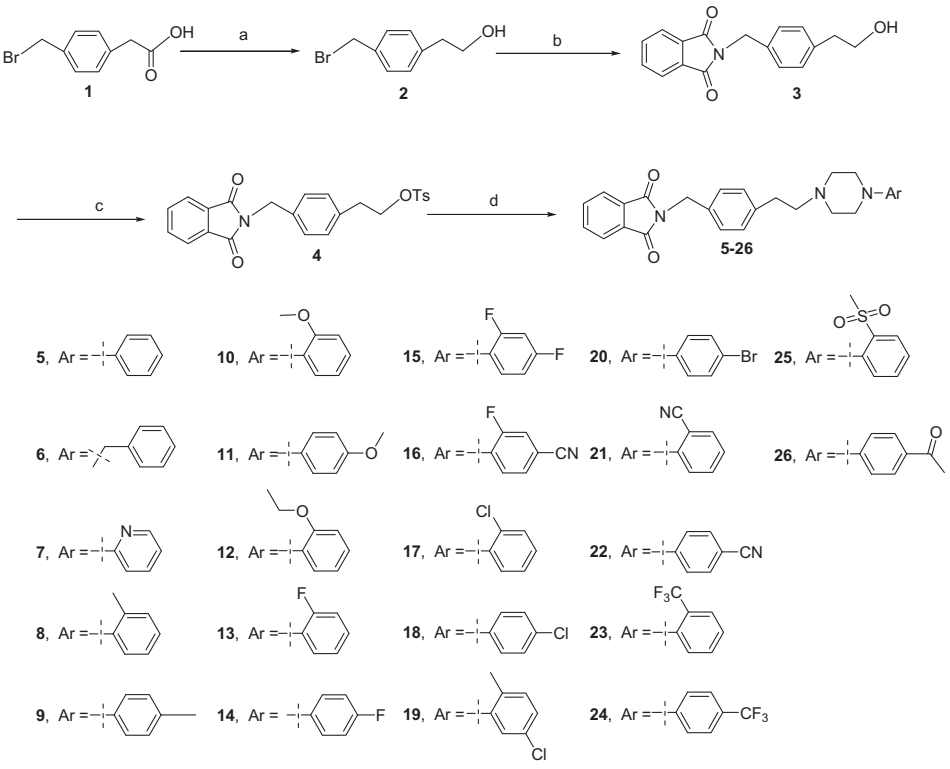

Scheme 1. Reagents and conditions: (a) $BH_3{\cdot}S(CH_3)_2$, THF, 0 °C for 1 h, and then room temperature for 10 h; (b) phthalimide potassium salt, K_2CO_3, CH_3CN, reflux, 16 h; (c) TsCl, Et_3N and 4-dimethylaminopyridine, CH_2Cl_2, 0 °C, 16 h; (d) arylpiperazines, K_2CO_3, CH_3CN, reflux, 16 h.

Table 1
Antagonistic activities (IC_{50}) on α_1-ARs (α_{1A}, α_{1B}, and α_{1D}) of **5–26**

Compd	IC_{50}[a] (nM)			Selectivity ratio	
	α_{1A}	α_{1B}	α_{1D}	α_{1B}/α_{1A}	α_{1B}/α_{1D}
5	151.30	875.30	1758.00	5.8	0.5
6	1200.00	1007.00	115.50	0.8	8.7
7	49.61	12.57	11.31	0.3	1.1
8	227.70	948.80	80550.00	4.2	0.01
9	2.03	28.91	343.60	14.2	0.08
10	30.12	100.90	1235.00	3.3	0.08
11	884.70	406.20	1862.00	0.5	0.2
12	32.43	433.30	239.90	13.4	1.8
13	96.01	1876.00	10630.00	19.5	0.2
14	229.40	684.00	122.00	3.0	5.6
15	89.94	787.50	493.30	8.8	1.6
16	128.00	34.76	957.20	0.3	0.04
17	15.16	781.50	36.62	51.5	21.3
18	551.90	794.40	35.16	1.4	22.6
19	34.47	31.62	31.28	0.9	1.0
20	3421.00	1003.00	7426.00	0.3	0.1
21	36.14	180.00	16.73	5.0	10.8
22	89.24	769.40	63.54	8.6	12.1
23	384.20	250.40	163.70	0.7	1.5
24	66.23	19.69	12.87	0.3	1.5
25	46.44	199.00	10.07	4.3	19.8
26	14.25	121.90	866.40	8.6	0.2
Naftopidil	555	634	55.2	11.53	114.8

[a] IC_{50} values are taken as means ± standard deviation from three experiments.

based on the common binding region of GPCRs. We found that Glu residue, the key amino acid residue on the pocket, was the residue responsible for ligand binding. The binding pockets of the three subtypes were similar, such as Phe289 from the π–π bond and Gln195 from the hydrogen bonding with ligands from their sequence alignment of the binding region. However, they still had their unique amino acids, respectively: Ile193 versus Val193 versus Ile193, Met293 versus Leu293 versus Leu293, and Lys302 versus Leu302 versus Leu302, and so on to α_{1A}, α_{1B} and α_{1D}. Moreover, the key amino residues around the binding pocket of the three subtypes were differentiated (Fig. 4). The conformations of Ile193 in α_{1A} and Val193 in α_{1B} were entirely different indicating that there was conformation difference of the same binding ligand. Ile193 in α_{1A}, which was closer to the binding pocket, exhibited hydrogen bonding interaction with the ligand; this phenomenon was unlikely to occur in α_{1B}. The different conformations of the same amino residues at the same region of the three subtypes can induce change in the active pocket conformation. Cys191 was the typical residue in that its stereo conformation in α_{1B} completely differed from those in α_{1A} and α_{1D}.

Considering compound **17** was confirmed with high affinity for $\alpha_{1A/1D}$-AR subtypes, approximately 51.5- and 21.3-fold higher potency was observed for α_{1A} and $_{1D}$ than for α_{1B}, respectively. The docking-binding mode of $\alpha_{1A/1D}$-AR and **17** were performed using Surflex-Dock (SYBYL) (Fig. 5). Compound **17** with a carbonyl group promoted intermolecular hydrogen bonding with ILE193

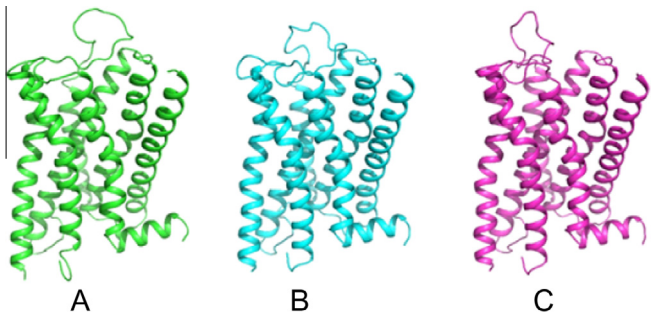

Figure 3. The models of α_1-ARs (A: 1A, B: 1B, and C: 1D).

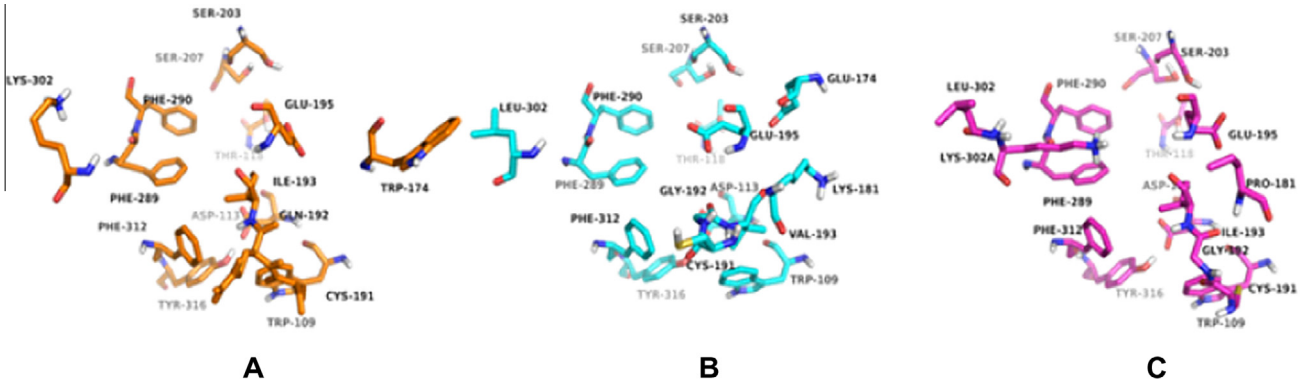

Figure 4. The key amino residues surrounded the α_1-ARs's pockets (3 Å, A: 1A, B: 1B, and C: 1D).

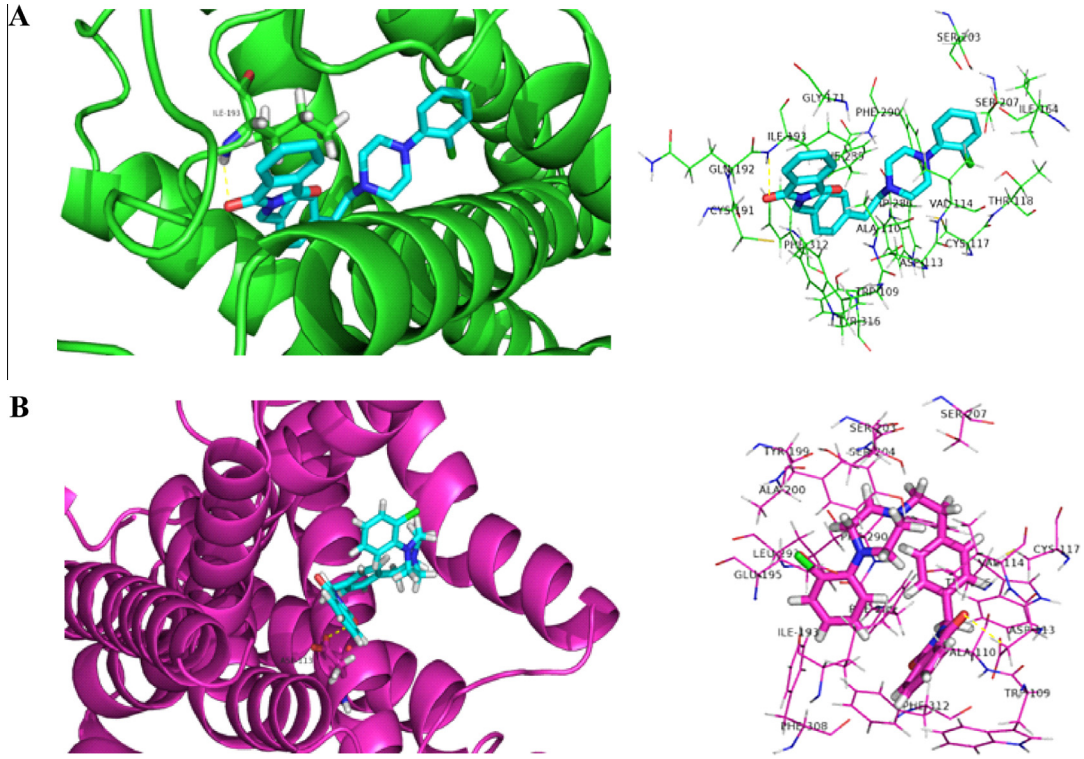

Figure 5. Molecular docking models of compound **17** inside active site (3 Å) of α_{1A}-AR (A) and α_{1D}-AR (B).

amino residue in α_{1A}-AR model, which was consistent with the perdition of binding sites of α_{1A}-AR. VAL114 was also reasonable for the binding mode of **17** and α_{1D}-AR by charge–charge interactions. The conformation of **17** was highly folded by charge–charge intramolecular interactions to match the pocket of α_{1D}-AR.

3. Conclusion

This study reported the synthesis and biological evaluation of a novel class of arylpiperazine derivatives. Some compounds exhibited strong antagonistic effects on α_{1A} and/or α_{1D} subtypes and better α_{1A} and/or α_{1D} subtype selectivity over α_{1B}. Compounds with a chloro (**17**) group at the *o*-position on the phenyl group or a cyano (**22**) group at the *p*-position demonstrated strong antagonistic effects on α_{1A} and α_{1D} subtypes, and better α_{1A} and α_{1D} subtypes selectivity over α_{1B}. The docking study of α_1-ARs with the most potent ligands (**17**) exhibited a good docking score and identified the important ILE193 residue to α_{1A}-AR. The docking study showed that hydrophobic interactions played an important role in the $\alpha_{1A/1D}$-AR ligand selectivity. This results provided by the binding-mode map can help elucidate the subtype selectivity and aid the design of high α_{1A} and/or α_{1D} subtype selective arylpiperazine derivatives in the future.

4. Experimental section

4.1. Chemistry

Reagents and solvents were commercially available. Solvents were dried and purified using standard procedures prior to use. Melting points were determined on a Fisher Johns hot-stage apparatus and are uncorrected. NMR spectra were determined on Bruker AV-400 NB spectrometer in $CDCl_3$ using TMS as internal standard, and coupling constants (*J*) are in Hz. EI mass spectra were

recorded on a DSQ mass spectrometer, and HRMS spectra were recorded on LTQ Orbitrap LC–MS (Thermo, Rockford, IL, USA). All derivatives tested for biological activity showed >95% putity by HPLC analysis (detection at 254 nm). Flash column chromatography was performed with silica gel (Qing Dao Ocean Chemical Factory, 300–400 mesh) eluted with petroleum ether–ethyl acetate.

4.1.1. 2-(4-(Bromomethyl)phenyl)ethanol (2)

To a cooled (0 °C) solution of carboxylic acid **1** (5 g, 0.021 mol) in dry tetrahydrofuran (THF, 100 mL) borane–dimethyl sulfide complex (21.9 mL, 0.042 mol, 2 M in THF) was added dropwise. The reaction mixture was stirred at 0 °C for 1 h and at room temperature for 10 h. Water (20 mL) was added slowly and extracted with ethyl acetate (3 × 100 mL). The combined organic phase was successively washed with water, brine, dried over anhydrous magnesium sulfate, and concentrated in vacuo. The resulting residue was directly used without further purification in the following step.

4.1.2. 2-(4-(2-Hydroxyethyl)benzyl)isoindoline-1,3-dione (3)

To a solution of compound **2** (4 g, 18.7 mmol) in acetone (100 mL) potassium phthalimide (3.46 g, 18.7 mmol) and potassium carbonate (2.58 g, 18.7 mmol) were added, and the reaction mixture was stirred at reflux for16 h. After cooling to ambient temperature, the reaction mixture was filtered through a Buchner funnel. After filtration the filtrate was concentrated in vacuo and the residue was purified by silica gel column chromatography using ethyl acetate/petroleum ether (1:8, v/v) as eluent to afford 4.31 g of compound **3**. White solid; mp 101.2–101.8 °C; yield, 70% (from compound **1**); ^{1}H NMR (400 MHz, $CDCl_3$) δ in ppm: 7.84 (dd, J = 5.5, 3.0 Hz, 2H), 7.70 (dd, J = 5.5, 3.0 Hz, 2H), 7.38 (d, J = 8.0 Hz, 2H), 7.17 (d, J = 8.0 Hz, 2H), 4.82 (s, 2H), 3.82 (t, J = 6.5 Hz, 2H), 2.83 (t, J = 6.5 Hz, 2H), 1.44 (s, 1H); ^{13}C NMR (101 MHz, $CDCl_3$) δ in ppm: 168.5, 138.6, 135.0, 134.4, 132.6, 129.7, 129.3, 123.7, 64.0, 41.7, 39.3; MS (EI) m/z: 281 (M^+), 251 (100%), 232, 204, 192, 178, 160.

4.1.3. 2-(4-((1,3-Dioxoisoindolin-2-yl)methyl)phenyl)ethyl-4-methylbenzenesulfonate (4)

To a solution of compound **3** (4 g, 14.2 mmol), triethylamine (5.75 g, 56.8 mmol) and 4-dimethylaminopyridine (0.17 g, 1.42 mmol) in dry dichloromethane (CH_2Cl_2, 100 mL) at 0 °C was added a solution of 4-toluene sulfonyl chloride (4.06 g, 21.3 mmol) in CH_2Cl_2 (10 mL) dropwise. The reaction mixture was stirred at 0 °C for 16 h.

Water (20 mL) was added slowly and extracted with CH_2Cl_2 (3 × 100 mL). The combined organic phase was successively washed with water, brine, dried over anhydrous magnesium sulfate, and concentrated in vacuo. The residue was purified by silica gel column chromatography using ethyl acetate/petroleum ether (1:10, v/v) as eluent to afford 5.88 g of compound **4**. White solid; mp 108.2–108.9 °C; yield, 95%; ^{1}H NMR (400 MHz, $CDCl_3$) δ in ppm: 7.84 (dd, J = 5.5, 3.0 Hz, 2H), 7.71 (dd, J = 5.5, 3.0 Hz, 2H), 7.66 (d, J = 8.3 Hz, 2H), 7.31 (d, J = 8.0 Hz, 2H), 7.28 (d, J = 8.3 Hz, 2H), 7.05 (d, J = 8.0 Hz, 2H), 4.81 (s, 2H), 4.16 (t, J = 7.0 Hz, 2H), 2.91 (t, J = 7.0 Hz, 2H), 2.42 (s, 3H); ^{13}C NMR (101 MHz, $CDCl_3$) δ in ppm: 168.4, 145.1, 136.3, 135.5, 134.4, 133.4, 132.6, 130.2, 129.6, 129.2, 128.3, 123.8, 70.8, 41.6, 35.4, 22.0; MS (EI) m/z: 435 (M^+), 363, 250 (100%), 235, 204, 178, 148.

4.1.4. General procedure for the synthesis of compounds 5–26

To a solution of **4** (100 mg, 0.23 mmol) in acetonitrile (CH_3CN, 10 mL) was added the corresponding arylpiperazines (1.2 equiv) and potassium carbonate (6.0 equiv). The reaction mixture was stirred at reflux for 16 h. After cooling to ambient temperature, the reaction mixture was filtered through a Buchner funnel. After filtration the filtrate was concentrated in vacuo and the residue was purified by silica gel column chromatography using ethyl acetate/petroleum ether (1:4, v/v) as eluent to afford the corresponding products, and all compounds were recrystallized from trichloromethane and *n*-hexane.

4.1.5. 2-(4-(2-(4-Phenylpiperazin-1-yl)ethyl)benzyl)isoindoline-1,3-dione (5)

White solid; mp 130.2–131.0 °C; yield, 95%; ^{1}H NMR (400 MHz, $CDCl_3$) δ in ppm: 7.84 (dd, J = 5.5, 3.0 Hz, 2H), 7.70 (dd, J = 5.5, 3.0 Hz, 2H), 7.37 (d, J = 8.0 Hz, 2H), 7.28–7.24 (m, 2H), 7.18 (d, J = 8.0 Hz, 2H), 6.93 (d, J = 8.0 Hz, 2H), 6.85 (t, J = 7.3 Hz, 1H), 4.82 (s, 2H), 3.22 (t, J = 5.0 Hz, 4H), 2.81 (dd, J = 9.8, 6.3 Hz, 2H), 2.67 (t, J = 5.0 Hz, 4H), 2.62 (dd, J = 9.8, 6.3 Hz, 2H); ^{13}C NMR (101 MHz, $CDCl_3$) δ in ppm: 168.1, 151.4, 140.0, 134.3, 134.0, 132.3, 129.2, 129.1, 128.9, 123.4, 119.8, 116.2, 60.4, 53.3, 49.3, 41.4, 33.3; HRMS (ESI) m/z [M+1]$^+$: calcd for $C_{27}H_{28}O_2N_3$, 426.2176, found, 426.2169.

4.1.6. 2-(4-(2-(4-Benzylpiperazin-1-yl)ethyl)benzyl)isoindoline-1,3-dione (6)

White solid; mp 122.8–123.4 °C; yield, 80%; ^{1}H NMR (400 MHz, $CDCl_3$) δ in ppm: 7.83 (dd, J = 5.5, 3.0 Hz, 2H), 7.69 (dd, J = 5.5, 3.0 Hz, 2H), 7.35 (d, J = 8.0 Hz, 2H), 7.31–7.28 (m, 5H), 7.14 (d, J = 8.0 Hz, 2H), 4.81 (s, 2H), 3.51 (s, 2H), 2.75 (dd, J = 9.8, 6.3 Hz, 2H), 2.66–2.38 (m, 10H); ^{13}C NMR (101 MHz, $CDCl_3$) δ in ppm: 168.1, 140.2, 138.3, 134.2, 134.0, 132.3, 129.3, 129.1, 128.8, 128.3, 127.1, 123.4, 63.2, 60.5, 53.3, 53.2, 41.4, 33.4; HRMS (ESI) m/z [M+1]$^+$: calcd for $C_{28}H_{30}O_2N_3$, 440.2332, found, 440.2327.

4.1.7. 2-(4-(2-(4-(Pyridin-2-yl)piperazin-1-yl)ethyl)benzyl) isoindoline-1,3-dione (7)

White solid; mp 123.0–123.4 °C; yield, 86.8%; ^{1}H NMR (400 MHz, $CDCl_3$) δ in ppm: 8.18 (dd, J = 5.0, 2.0 Hz, 1H), 7.83 (dd, J = 5.5, 3.0 Hz, 2H), 7.69 (dd, J = 5.5, 3.0 Hz, 2H), 7.46 (m, 1H), 7.36 (d, J = 8.0 Hz, 2H), 7.17 (d, J = 8.0 Hz, 2H), 6.63 (d, J = 8.8, 1H), 6.60 (dd, J = 7.2, 5.0 Hz, 1H), 4.82 (s, 2H), 3.57 (t, J = 5.0 Hz, 4H), 2.81 (dd, J = 9.8, 6.3 Hz, 2H), 2.64–2.59 (m, 6H); ^{13}C NMR (101 MHz, $CDCl_3$) δ in ppm: 168.4, 160.0, 148.4, 140.3, 137.8, 134.6, 134.4, 132.6, 129.4, 129.2, 123.7, 113.7, 107.5, 60.8, 53.4, 45.6, 41.8, 33.6; HRMS (ESI) m/z [M+1]$^+$: calcd for $C_{26}H_{27}O_2N_4$, 427.2128, found, 427.2130.

4.1.8. 2-(4-(2-(4-*o*-Tolylpiperazin-1-yl)ethyl)benzyl)isoindoline-1,3-dione (8)

White solid; mp 120.8–121.6 °C; yield, 87%; ^{1}H NMR (400 MHz, $CDCl_3$) δ in ppm: 7.84 (dd, J = 5.5, 3.0 Hz, 2H), 7.70 (dd, J = 5.5, 3.0 Hz, 2H), 7.37 (d, J = 8.0 Hz, 2H), 7.19–7.14 (m, 4H), 7.06–6.95 (m, 2H), 4.83 (s, 2H), 2.97 (t, J = 5.0 Hz, 4H), 2.82 (dd, J = 9.8, 6.3 Hz, 2H), 2.68 (br t, 4H), 2.64 (dd, J = 9.8, 6.3 Hz, 2H), 2.30 (s, 3H); ^{13}C NMR (101 MHz, $CDCl_3$) δ in ppm: 168.1, 151.6, 140.1, 134.3, 134.0, 132.7, 132.3, 131.1, 129.1, 128.9, 126.7, 123.4, 123.2, 119.1, 60.6, 53.8, 51.8, 41.5, 33.4, 18.0; HRMS (ESI) m/z [M+1]$^+$: calcd for $C_{28}H_{30}O_2N_3$, 440.2333, found, 440.2326.

4.1.9. 2-(4-(2-(4-*p*-Tolylpiperazin-1-yl)ethyl)benzyl)isoindoline-1,3-dione (9)

Light yellow solid; mp 150.4–151.1 °C; yield, 45%; ^{1}H NMR (400 MHz, $CDCl_3$) δ in ppm: 7.84 (dd, J = 5.5, 3.0 Hz, 2H), 7.70 (dd, J = 5.5, 3.0 Hz, 2H), 7.37 (d, J = 8.0 Hz, 2H), 7.17 (d, J = 8.0 Hz, 2H), 7.07 (d, J = 8.6 Hz, 2H), 6.85 (d, J = 8.6 Hz, 2H), 4.82 (s, 2H), 3.17 (t, J = 5.0 Hz, 4H), 2.81 (dd, J = 9.8, 6.3 Hz, 2H), 2.67 (t, J = 5.0 Hz, 4H), 2.62 (dd, J = 9.8, 6.3 Hz, 2H), 2.27 (s, 3H); ^{13}C NMR (101 MHz, $CDCl_3$) δ in ppm: 169.4, 150.6, 141.3, 135.5, 135.3, 133.5, 130.9, 130.5, 130.3, 130.1, 124.6, 117.7, 61.7, 54.6, 51.0,

42.7, 34.6, 21.7; HRMS (ESI) m/z [M+1]$^+$: calcd for $C_{28}H_{30}O_2N_3$, 440.2332, found, 440.2324.

4.1.10. 2-(4-(2-(4-(2-Methoxyphenyl)piperazin-1-yl)ethyl) benzyl)isoindoline-1,3-dione (10)

White solid; mp 132.8–133.6 °C; yield, 83%; ^{1}H NMR (400 MHz, $CDCl_3$) δ in ppm: 7.84 (dd, J = 5.5, 3.0 Hz, 2H), 7.70 (dd, J = 5.5, 3.0 Hz, 2H), 7.37 (d, J = 8.0 Hz, 2H), 7.18 (d, J = 8.0 Hz, 2H), 7.02–6.85 (m, 4H), 4.82 (s, 2H), 3.86 (s, 3H), 3.12 (br t, 4H), 2.82 (dd, J = 9.8, 6.3 Hz, 2H), 2.73 (br t, 4H), 2.64 (dd, J = 9.8, 6.3 Hz, 2H); ^{13}C NMR (101 MHz, $CDCl_3$) δ in ppm: 168.1, 152.4, 141.5, 140.1, 134.3, 134.0, 132.3, 129.1, 128.9, 123.4, 123.0, 121.1, 118.3, 111.4, 60.5, 55.5, 53.5, 50.7, 41.5, 33.3; HRMS (ESI) m/z [M+1]$^+$: calcd for $C_{28}H_{30}O_3N_3$, 456.2282, found, 456.2273.

4.1.11. 2-(4-(2-(4-(4-Methoxyphenyl)piperazin-1-yl)ethyl) benzyl)isoindoline-1,3-dione (11)

Light yellow solid; mp 142.6–143.6 °C; yield, 71.7%; ^{1}H NMR (400 MHz, $CDCl_3$) δ in ppm: 7.84 (dd, J = 5.5, 3.0 Hz, 2H), 7.69 (dd, J = 5.5, 3.0 Hz, 2H), 7.37 (d, J = 8.0 Hz, 2H), 7.17 (d, J = 8.0 Hz, 2H), 6.92–6.81 (m, 4H), 4.82 (s, 2H), 3.76 (s, 3H), 3.11 (t, J = 5.0 Hz, 4H), 2.81 (dd, J = 9.8, 6.3 Hz, 2H), 2.67 (t, J = 5.0 Hz, 4H), 2.62 (dd, J = 9.8, 6.3 Hz, 2H); ^{13}C NMR (101 MHz, $CDCl_3$) δ in ppm: 168.1, 153.9, 145.9, 140.1, 134.3, 134.0, 132.3, 129.1, 128.9, 123.4, 118.3, 114.6, 60.4, 55.7, 53.4, 50.7, 41.4, 33.4; HRMS (ESI) m/z [M+1]$^+$: calcd for $C_{28}H_{30}O_3N_3$, 456.2281, found, 456.2273.

4.1.12. 2-(4-(2-(4-(2-Ethoxyphenyl)piperazin-1-yl)ethyl)benzyl) isoindoline-1,3-dione (12)

White solid; mp 122.4–123.1 °C; yield, 86%; ^{1}H NMR (400 MHz, $CDCl_3$) δ in ppm: 7.84 (dd, J = 5.5, 3.0 Hz, 2H), 7.69 (dd, J = 5.5, 3.0 Hz, 2H), 7.37 (d, J = 8.0 Hz, 2H), 7.18 (d, J = 8.0 Hz, 2H), 6.98–6.83 (m, 4H), 4.82 (s, 2H), 4.07 (q, J = 7.0 Hz, 2H), 3.15 (br t, 4H), 2.82 (dd, J = 9.8, 6.3 Hz, 2H), 2.72 (br t, 4H), 2.64 (dd, J = 9.8, 6.3 Hz, 2H), 1.45 (t, J = 7.0 Hz, 3H); ^{13}C NMR (101 MHz, $CDCl_3$) δ in ppm: 168.4, 152.0, 141.8, 140.4, 134.6, 134.3, 132.6, 129.4, 129.2, 123.7, 123.1, 121.4, 118.6, 113.0, 64.0, 60.9, 53.8, 50.9, 41.8, 33.6, 15.4; HRMS (ESI) m/z [M+1]$^+$: calcd for $C_{29}H_{32}O_3N_3$, 470.2438, found, 470.2432.

4.1.13. 2-(4-(2-(4-(2-Fluorophenyl)piperazin-1-yl)ethyl)benzyl) isoindoline-1,3-dione (13)

White solid; mp 133.6–134.1 °C; yield, 82%; ^{1}H NMR (400 MHz, $CDCl_3$) δ in ppm: 7.84 (dd, J = 5.5, 3.0 Hz, 2H), 7.69 (dd, J = 5.5, 3.0 Hz, 2H), 7.37 (d, J = 8.0 Hz, 2H), 7.18 (d, J = 8.0 Hz, 2H), 7.08–6.89 (m, 4H), 4.82 (s, 2H), 3.14 (t, J = 5.0 Hz, 4H), 2.81 (dd, J = 9.8, 6.3 Hz, 2H), 2.70 (t, J = 5.0 Hz, 4H), 2.63 (dd, J = 9.8, 6.3 Hz, 2H); ^{13}C NMR (101 MHz, $CDCl_3$) δ in ppm: 168.1, 157.1, 154.6, 140.3, 140.2, 140.0, 134.3, 134.0, 132.3, 129.1, 128.9, 124.6, 124.5, 123.4, 122.5, 122.5, 119.0, 119.0, 116.3, 116.1, 60.4, 53.4, 50.6, 41.4, 33.3; HRMS (ESI) m/z [M+1]$^+$: calcd for $C_{27}H_{27}O_2N_3F$, 444.2082, found, 444.2075.

4.1.14. 2-(4-(2-(4-(4-Fluorophenyl)piperazin-1-yl)ethyl)benzyl) isoindoline-1,3-dione (14)

Light yellow solid; mp 152.0–152.6 °C; yield, 59%; ^{1}H NMR (400 MHz, $CDCl_3$) δ in ppm: 7.84 (dd, J = 5.5, 3.0 Hz, 2H), 7.70 (dd, J = 5.5, 3.0 Hz, 2H), 7.37 (d, J = 8.0 Hz, 2H), 7.17 (d, J = 8.0 Hz, 2H), 6.98–6.85 (m, 4H), 4.82 (s, 2H), 3.14 (t, J = 5.0 Hz, 4H), 2.80 (dd, J = 9.8, 6.3 Hz, 2H), 2.66 (t, J = 5.0 Hz, 4H), 2.62 (dd, J = 9.8, 6.3 Hz, 2H); ^{13}C NMR (101 MHz, $CDCl_3$) δ in ppm: 169.4, 159.7, 157.3, 149.3, 141.2, 135.5, 135.3, 133.5, 130.3, 130.1, 124.6, 119.2, 119.1, 116.9, 116.7, 61.6, 54.5, 51.5, 42.7, 34.6; HRMS (ESI) m/z [M+1]$^+$: calcd for $C_{27}H_{27}O_2N_3F$, 444.2081, found, 444.2075.

4.1.15. 2-(4-(2-(4-(2,4-Difluorophenyl)piperazin-1-yl)ethyl) benzyl)isoindoline-1,3-dione (15)

White solid; mp 122.4–123.0 °C; yield, 75.5%; ^{1}H NMR (400 MHz, $CDCl_3$) δ in ppm: 7.84 (dd, J = 5.5, 3.0 Hz, 2H), 7.70 (dd, J = 5.5, 3.0 Hz, 2H), 7.37 (d, J = 8.0 Hz, 2H), 7.17 (d, J = 8.0 Hz, 2H), 6.93–6.86 (m, 1H), 6.83–6.76 (m, 2H), 4.82 (s, 2H), 3.07 (t, J = 5.0 Hz, 4H), 2.80 (dd, J = 9.8, 6.3 Hz, 2H), 2.69 (t, J = 5.0 Hz, 4H), 2.63 (dd, J = 9.8, 6.3 Hz, 2H); HRMS (ESI) m/z [M+1]$^+$: calcd for $C_{27}H_{26}O_2N_3F_2$, 462.1988, found, 462.1982.

4.1.16. 4-(4-(2-(4-((1,3-Dioxoisoindolin-2-yl)methyl)phenyl) ethyl)piperazin-1-yl)-3-fluorobenzonitrile (16)

White solid; mp 170.3–171.3 °C; yield, 46.5%; ^{1}H NMR (400 MHz, $CDCl_3$) δ in ppm: 7.84 (dd, J = 5.5, 3.0 Hz, 2H), 7.70 (dd, J = 5.5, 3.0 Hz, 2H), 7.37–7.33 (m, 3H), 7.24 (dd, J = 2.0, 2.0 Hz, 1H), 7.16 (d, J = 8.0 Hz, 2H), 6.90 (t, J = 8.4 Hz, 1H), 4.82 (s, 2H), 3.24 (t, J = 5.0 Hz, 4H), 2.80 (dd, J = 9.8, 6.3 Hz, 2H), 2.67 (t, J = 5.0 Hz, 4H), 2.63 (dd, J = 9.8, 6.3 Hz, 2H); ^{13}C NMR (101 MHz, $CDCl_3$) δ in ppm: 169.3, 156.5, 154.1, 145.5, 145.4, 141.0, 135.6, 135.3, 133.5, 130.7, 130.3, 130.1, 124.6, 121.1, 120.9, 120.0, 120.0, 119.7, 104.9, 104.8, 61.4, 54.2, 51.0, 50.9, 42.6, 34.5; HRMS (ESI) m/z [M+1]$^+$: calcd for $C_{28}H_{26}O_2N_4F$, 469.2034, found, 469.2025.

4.1.17. 2-(4-(2-(4-(2-Chlorophenyl)piperazin-1-yl)ethyl)benzyl) isoindoline-1,3-dione (17)

White solid; mp 147.7–148.1 °C; yield, 86%; ^{1}H NMR (400 MHz, $CDCl_3$) δ in ppm: 7.84 (dd, J = 5.5, 3.0 Hz, 2H), 7.70 (dd, J = 5.5, 3.0 Hz, 2H), 7.38–7.34 (m, 3H), 7.24–7.16 (m, 3H), 7.05 (dd, J = 8.0, 1.5 Hz, 1H), 6.96 (td, J = 8.0, 1.5 Hz, 1H), 4.82 (s, 2H), 3.10 (br t, 4H), 2.81 (dd, J = 9.8, 6.3 Hz, 2H), 2.71 (br t, 4H), 2.64 (dd, J = 9.8, 6.3 Hz, 2H); ^{13}C NMR (101 MHz, $CDCl_3$) δ in ppm: 169.4, 150.6, 141.3, 135.5, 135.3, 133.5, 132.0, 130.3, 130.1, 130.1, 128.9, 125.0, 124.6, 121.7, 61.7, 54.7, 52.5, 42.7, 34.6; HRMS (ESI) m/z [M+1]$^+$: calcd for $C_{27}H_{27}O_2N_3Cl$, 460.1786, found, 460.1782.

4.1.18. 2-(4-(2-(4-(4-Chlorophenyl)piperazin-1-yl)ethyl)benzyl) isoindoline-1,3-dione (18)

Light yellow solid; mp 160.0–160.6 °C; yield, 73.9%; ^{1}H NMR (400 MHz, $CDCl_3$) δ in ppm: 7.84 (dd, J = 5.5, 3.0 Hz, 2H), 7.70 (dd, J = 5.5, 3.0 Hz, 2H), 7.36 (d, J = 8.0 Hz, 2H), 7.19 (dd, J = 7.2, 2.4 Hz, 2H), 7.17 (d, J = 8.0 Hz, 2H), 6.83 (dd, J = 7.2, 2.4 Hz, 2H), 4.82 (s, 2H), 3.18 (t, J = 5.0 Hz, 4H), 2.80 (dd, J = 9.8, 6.3 Hz, 2H), 2.65 (t, J = 5.0 Hz, 4H), 2.62 (dd, J = 9.8, 6.3 Hz, 2H); ^{13}C NMR (101 MHz, $CDCl_3$) δ in ppm: 169.4, 151.3, 141.2, 135.6, 135.3, 133.5, 130.3, 130.3, 130.1, 125.8, 124.6, 118.5, 61.5, 54.4, 50.5, 42.7, 34.5; HRMS (ESI) m/z [M+1]$^+$: calcd for $C_{27}H_{27}O_2N_3Cl$, 460.1786, found, 460.1782.

4.1.19. 2-(4-(2-(4-(5-Chloro-2-methylphenyl)piperazin-1-yl) ethyl)benzyl)isoindoline-1,3-dione (19)

White solid; mp 183.8–184.7 °C; yield, 80%; ^{1}H NMR (400 MHz, $CDCl_3$) δ in ppm: 7.84 (dd, J = 5.5, 3.0 Hz, 2H), 7.70 (dd, J = 5.5, 3.0 Hz, 2H), 7.37 (d, J = 8.0 Hz, 2H), 7.18 (d, J = 8.0 Hz, 2H), 7.07 (d, J = 8.0 Hz, 1H), 6.97 (d, J = 2.0 Hz, 1H), 6.94 (dd, J = 8.0, 2.0 Hz, 1H), 4.82 (s, 2H), 2.94 (t, J = 5.0 Hz, 4H), 2.81 (dd, J = 9.8, 6.3 Hz, 2H), 2.66 (br t, 4H), 2.64 (dd, J = 9.8, 6.3 Hz, 2H), 2.24 (s, 3H); ^{13}C NMR (101 MHz, $CDCl_3$) δ in ppm: 169.4, 153.9, 141.2, 135.5, 135.3, 133.5, 133.2, 133.1, 132.1, 130.3, 130.1, 124.6, 124.3, 120.8, 61.6, 54.8, 52.8, 42.7, 34.5, 18.8; HRMS (ESI) m/z [M+1]$^+$: calcd for $C_{28}H_{29}O_2N_3Cl$, 474.1942, found, 474.1938.

4.1.20. 2-(4-(2-(4-(4-Bromophenyl)piperazin-1-yl)ethyl)benzyl) isoindoline-1,3-dione (20)

Light yellow solid; mp 167.4–167.9 °C; yield, 70%; ^{1}H NMR (400 MHz, $CDCl_3$) δ in ppm: 7.84 (dd, J = 5.5, 3.0 Hz, 2H), 7.70

(dd, J = 5.5, 3.0 Hz, 2H), 7.36 (d, J = 8.0 Hz, 2H), 7.33 (dd, J = 6.8, 2.0 Hz, 2H), 7.17 (d, J = 8.0 Hz, 2H), 6.78 (dd, J = 6.8, 2.0 Hz, 2H), 4.82 (s, 2H), 3.17 (t, J = 5.0 Hz, 4H), 2.79 (dd, J = 9.8, 6.3 Hz, 2H), 2.64 (t, J = 5.0 Hz, 4H), 2.61 (dd, J = 9.8, 6.3 Hz, 2H); ^{13}C NMR (101 MHz, $CDCl_3$) δ in ppm: 168.1, 150.4, 140.0, 134.3, 134.1, 132.3, 132.0, 129.1, 128.9, 123.4, 117.7, 111.9, 60.3, 53.1, 49.1, 41.4, 33.3; HRMS (ESI) m/z $[M+1]^+$: calcd for $C_{27}H_{27}O_2N_3Br$, 504.1281, found, 504.1271.

4.1.21. 2-(4-(2-(4-(2-Isocyanophenyl)piperazin-1-yl)ethyl) benzyl)isoindoline-1,3-dione (21)

White solid; mp 141.7–142.2 °C; yield, 82.8%; ^{1}H NMR (400 MHz, $CDCl_3$) δ in ppm: 7.84 (dd, J = 5.5, 3.0 Hz, 2H), 7.70 (dd, J = 5.5, 3.0 Hz, 2H), 7.55 (dd, J = 8.0, 1.3 Hz, 1H), 7.47 (m, 1H), 7.37 (d, J = 8.0 Hz, 2H), 7.17 (d, J = 8.0 Hz, 2H), 7.01–6.98 (m, 2H), 4.82 (s, 2H), 3.26 (t, J = 5.0, 4H), 2.81 (dd, J = 9.8, 6.3 Hz, 2H), 2.74 (t, J = 5.0, 4H), 2.65 (dd, J = 9.8, 6.3 Hz, 2H); ^{13}C NMR (101 MHz, $CDCl_3$) δ in ppm: 168.1, 155.8, 139.9, 134.5, 134.3, 134.0, 133.9, 132.3, 129.1, 128.9, 123.4, 121.8, 118.8, 118.5, 106.1, 60.2, 53.2, 51.6, 41.4, 33.3; HRMS (ESI) m/z $[M+1]^+$: calcd for $C_{28}H_{27}O_2N_4$, 451.2128, found, 451.2122.

4.1.22. 4-(4-(2-(4-((1,3-Dioxoisoindolin-2-yl)methyl)phenyl) ethyl)piperazin-1-yl)benzonitrile (22)

Light yellow solid; mp 150.0–150.8 °C; yield, 48.4%; ^{1}H NMR (400 MHz, $CDCl_3$) δ in ppm: 7.83 (dd, J = 5.5, 3.0 Hz, 2H), 7.70 (dd, J = 5.5, 3.0 Hz, 2H), 7.48 (d, J = 9.0 Hz, 2H), 7.36 (d, J = 8.0 Hz, 2H), 7.16 (d, J = 8.0 Hz, 2H), 6.84 (d, J = 9.0 Hz, 2H), 4.82 (s, 2H), 3.33 (t, J = 5.0 Hz, 4H), 2.79 (dd, J = 9.8, 6.3 Hz, 2H), 2.64–2.59 (m, 6H); ^{13}C NMR (101 MHz, $CDCl_3$) δ in ppm: 169.3, 154.7, 141.0, 135.6, 135.3, 134.9, 134.8, 133.5, 130.3, 130.1, 124.6, 121.3, 115.5, 101.6, 61.4, 54.0, 48.5, 42.6, 34.5; HRMS (ESI) m/z $[M+1]^+$: calcd for $C_{28}H_{27}O_2N_4$, 451.2128, found, 451.2127.

4.1.23. 2-(4-(2-(4-(2-(Trifluoromethyl)phenyl)piperazin-1-yl) ethyl)benzyl)isoindoline-1,3-dione (23)

White solid; mp 141.3–142.3 °C; yield, 79.4%; ^{1}H NMR (400 MHz, $CDCl_3$) δ in ppm: 7.84 (dd, J = 5.5, 3.0 Hz, 2H), 7.70 (dd, J = 5.5, 3.0 Hz, 2H), 7.61 (dd, J = 7.8, 0.8 Hz, 1H), 7.51 (t, J = 7.8 Hz, 1H), 7.51 (d, J = 7.8 Hz, 1H), 7.37 (d, J = 8.0 Hz, 2H), 7.22 (d, J = 7.8 Hz, 1H), 7.17 (d, J = 8.0 Hz, 2H), 4.82 (s, 2H), 2.98 (t, J = 5.0 Hz, 4H), 2.81 (dd, J = 10.0, 6.2 Hz, 2H), 2.68–2.62 (m, 6H); ^{13}C NMR (101 MHz, $CDCl_3$) δ in ppm: 168.1, 152.7, 140.1, 134.3, 134.0, 132.8, 132.3, 129.1, 128.9, 127.3, 127.3, 124.8, 124.1, 123.4, 60.5, 53.6, 53.5, 41.5, 33.4; HRMS (ESI) m/z $[M+1]^+$: calcd for $C_{28}H_{27}O_2N_3F_3$, 494.2049, found, 494.2041.

4.1.24. 2-(4-(2-(4-(4-(Trifluoromethyl)phenyl)piperazin-1-yl) ethyl)benzyl)isoindoline-1,3-dione (24)

Light yellow solid; mp 164.3–164.9 °C; yield, 48.5%; ^{1}H NMR (400 MHz, $CDCl_3$) δ in ppm: 7.84 (dd, J = 5.5, 3.0 Hz, 2H), 7.70 (dd, J = 5.5, 3.0 Hz, 2H), 7.47 (d, J = 8.7 Hz, 2H), 7.37 (d, J = 8.0 Hz, 2H), 7.17 (d, J = 8.0 Hz, 2H), 6.91 (d, J = 8.7 Hz, 2H), 4.82 (s, 2H), 3.33 (t, J = 5.0 Hz, 4H), 2.80 (dd, J = 9.8, 6.3 Hz, 2H), 2.66–2.60 (m, 6H); ^{13}C NMR (101 MHz, $CDCl_3$) δ in ppm: 168.5, 153.7, 140.2, 134.7, 134.4, 132.6, 129.4, 129.2, 126.8, 126.8, 123.7, 114.9, 60.6, 53.3, 48.4, 41.8, 33.6; HRMS (ESI) m/z $[M+1]^+$: calcd for $C_{28}H_{27}O_2N_3F_3$, 494.2049, found, 494.2040.

4.1.25. 2-(4-(2-(4-(2-(Methylsulfonyl)phenyl)piperazin-1-yl) ethyl)benzyl)isoindoline-1,3-dione (25)

White solid; mp 228.5–229.4 °C; yield, 73.5%; ^{1}H NMR (400 MHz, $CDCl_3$) δ in ppm: 8.07 (dd, J = 8.0, 1.6 Hz, 1H), 7.84 (dd, J = 5.5, 3.0 Hz, 2H), 7.70 (dd, J = 5.5, 3.0 Hz, 2H), 7.61 (td, J = 8.0, 1.6 Hz, 1H), 7.41 (dd, J = 8.0, 0.8 Hz, 1H), 7.37 (d, J = 8.0 Hz, 2H), 7.32 (td, J = 8.0, 0.8 Hz, 1H), 7.17 (d, J = 8.0 Hz, 2H), 4.82 (s, 2H), 3.33 (s, 3H), 3.12 (br t, 4H), 2.81 (dd, J = 9.8, 6.3 Hz, 2H), 2.72 (br t, 4H), 2.65 (dd, J = 9.8, 6.3 Hz, 2H); ^{13}C NMR (101 MHz, $CDCl_3$) δ in ppm: 168.4, 152.9, 140.2, 137.5, 135.1, 134.7, 134.4, 132.6, 130.3, 129.4, 129.2, 126.0, 124.3, 123.7, 60.7, 54.1, 54.0, 43.2, 41.7, 33.6; HRMS (ESI) m/z $[M+1]^+$: calcd for $C_{28}H_{30}O_4N_3S$, 504.1951, found, 504.1941.

4.1.26. 2-(4-(2-(4-(4-Acetylphenyl)piperazin-1-yl)ethyl)benzyl) isoindoline-1,3-dione (26)

Light yellow solid; mp 157.4–157.8 °C; yield, 55.9%; ^{1}H NMR (400 MHz, $CDCl_3$) δ in ppm: 7.87 (d, J = 9.0 Hz, 2H), 7.84 (dd, J = 5.5, 3.0 Hz, 2H), 7.70 (dd, J = 5.5, 3.0 Hz, 2H), 7.36 (d, J = 8.0 Hz, 2H), 7.17 (d, J = 8.0 Hz, 2H), 6.86 (d, J = 9.0 Hz, 2H), 4.82 (s, 2H), 3.38 (t, J = 5.0 Hz, 4H), 2.81 (dd, J = 9.8, 6.3 Hz, 2H), 2.65–2.61 (m, 6H), 2.51 (s, 3H); ^{13}C NMR (101 MHz, $CDCl_3$) δ in ppm: 197.8, 169.4, 155.4, 135.6, 135.3, 133.5, 131.7, 130.3, 130.1, 129.0, 124.6, 114.7, 61.5, 54.1, 48.6, 42.6, 34.5, 27.4; HRMS (ESI) m/z $[M+1]^+$: calcd for $C_{29}H_{30}O_3N_3$, 468.2281, found, 468.2273.

4.2. Dual-luciferase reporter gene assay

Firefly and Renilla luciferase activities, which are indicated as RLUs, were determined using Dual-Glo luciferase assay kits (Promega) according to the manufacturer's instructions. RLUs were measured using a luminometer (GloMaxTM 96-Microplate Luminometer, Promega) and are reported as the mean ± SEM of three individual experiments. For agonists, fold of induction = $LU_{induced}$/$RLU_{uninduced}$. For antagonists, % of control = 100 × RLU (agonist + antagonist)/RLU (agonist alone). All RLUs were normalized against firefly RLUs/Renilla RLUs. Data are expressed as EC_{50}/IC_{50} values in μM, and the IC_{50} of phenylephrine (μM) was calculated by plotting the data using nonlinear regression analysis in GraphPad Prism 5 software.

4.3. Homology model building of α_1-ARs and molecular docking studies

The structure of α_1-ARs is difficult to elucidate because of lack of X-ray diffraction structural data.[22] The sequence of the three α_1-AR subtypes (SwissProt α_{1A}-AR: P35348; α_{1B}-AR: P35368; and α_{1D}-AR: P25100) were based to predict the membrane protein and TM region within the SOSUI program.[23] Protein blast was used to search the template protein. β_2-Adrenergic G protein-coupled receptor (Protein code: 2RH1) was the best match to the α_{1A}-, α_{1B}-, and α_{1D}-AR subtypes; these sequence identity obtained for the three α_1-AR subtypes were 36%, 35% and 38%, respectively[24] (Supplementary data in Fig. S1). The models of the three α_1-ARs were built using homology modeling protocol (Prime, Schrodinger); the diffusible ligand carazolol in the crystal structure of β_2-adrenergic receptor (β_2-AR) was chosen for the study of receptor–ligand interactions.[25,26] The three models were refined using energy minimization with macromodel (Schrodinger) by (a) fixing the main chain and refining the side chains by 500 steps; (b) fixing the side chains and refining the main chain by 500 steps; and (c) refining the whole body by 500 steps in a simulated octanol environment. 3D Ranachandran plots and profiles were obtained to evaluate the model structures. For the crystal structure of β_2-AR, the intracellular loop region 3 (IL3) was replaced by T4 lysozyme to increase the solubility and stability of the receptor, and the active site of the GPCRs was located in the extracellular region near loop 2 (EL2). IL3 loop was removed in the modeling process of the three targets since this loop was unlikely to play a major role in ligand binding. The highly conserved disulfide bond, DRY region in loop 3, NPxxY in loop 7, and CWxP in loop 6 were retained in the models.

Molecular docking was performed using Surflex-Dock (SYBYL®8.1 molecular modeling software). The diffusible ligand

carazolol in the crystal structure of β_2-adrenergic receptor (β_2-AR) was retained as reference ligand in order to study the α_1-ARs–ligand interactions. Molecule was sketched and minimized using Powell optimization in the presence of the Tripos force field with a convergence criterion of 0.001 kcal/mol Å and then assigned with the Gasteiger–Hückel charges. Automatic docking was employed. Other parameters were established by default in software.

Acknowledgments

This part of research were funded by The National Science Foundation of Guangdong Province (Grant 2015A030313464 to F. X., S2013040014088 to H.C.), and Science Foundation of Zhejiang Province, China (Grant LY12B02008 to F.X.). We acknowledge the technical assistance of Experimental Medical Research Center, Guangzhou Medical University.

Supplementary data

Supplementary data associated with this article can be found, in the online version, at http://dx.doi.org/10.1016/j.bmc.2015.11.020.

References and notes

1. Nanda, K.; Naruganaphalli, K. S.; Gupta, S.; Malhotra, S.; Tiwari, A.; Hegde, L. G.; Jain, S.; Sinha, N.; Gupta, J. B.; Chugh, A.; Anand, N.; Ray, A. *Eur. J. Pharmacol.* **2009**, *607*, 213.
2. Carrieri, A.; Piergentili, A.; Del-Bello, F.; Giannella, M.; Pigini, M.; Leonardi, A.; Fanelli, F.; Quaglia, W. *Bioorg. Med. Chem.* **2010**, *18*, 7065.
3. Sato, S. C.; Hatanaka, T.; Yuyama, H.; Ukai, M.; Noguchi, Y.; Ohtake, A.; Taguchi, K.; Sasamata, M.; Miyata, K. *Biol. Pharm. Bull.* **2012**, *35*, 72.
4. Lepor, H.; Henry, D.; Laddu, A. R. *Prostate* **1991**, *18*, 345.
5. Bendix-Holme, J.; Christensen, M. M.; Rasmussen, P. C.; Jacobsen, F.; Nielsen, J.; Norgaard, J. P.; Olesen, S.; Noer, L.; Wolf, H.; Elkjaer-Husted, S. *Scand. J. Urol. Nephrol.* **1994**, *28*, 77.
6. Jardin, A.; Bensadoun, H.; Delauche-Cavallier, M. C.; Stalla-Bourdillon, A.; Attali, P. *Br. J. Urol.* **1984**, *74*, 579.
7. Wong, W. C.; Chiu, G.; Wetzel, J. M.; Marzabadi, M. R.; Nagarathnam, D.; Wang, D.; Fang, J.; Miao, S. W.; Forray, C.; Vaysse, P. J.; Branchek, T. A.; Gluchowski, C.; Tang, R.; Lepor, H. *J. Med. Chem.* **1998**, *41*, 2643.
8. Lepor, H. *Urology* **1995**, *45*, 406.
9. Djavan, B.; Marberger, M. *Eur. Urol.* **1999**, *36*, 1.
10. Dellabella, M.; Milanese, G.; Muzzonigro, G. *J. Urol.* **2003**, *170*, 2202.
11. Morita, T.; Wada, I.; Saeki, H.; Tsuchida, S.; Weiss, R. M. *J. Urol.* **1987**, *137*, 132.
12. Nishino, Y.; Masue, T.; Miwa, K.; Takahashi, Y.; Ishihara, S.; Deguchi, T. *BJU Int.* **2006**, *97*, 747.
13. Kojima, Y.; Sasaki, S.; Kubota, Y.; Hayase, M.; Hayashi, Y.; Shinoura, H.; Tsujimoto, G.; Kohri, K. *J. Urol.* **2008**, *179*, 1040.
14. Paluchowska, M. H.; Mokrosz, M. J.; Bojarski, A.; Wesolowska, A.; Borycz, J.; Charakchieva-Minol, S.; Chojnacka-Wojcik, E. *J. Med. Chem.* **1999**, *42*, 4952.
15. Raghupathi, R. K.; Rydelek-Fitzgerald, L.; Teitler, M.; Glennon, R. A. *J. Med. Chem.* **1991**, *34*, 2633.
16. Orjales, A.; Alonso-Cires, L.; Labeaga, L.; Corcostegui, R. *J. Med. Chem.* **1995**, *38*, 1273.
17. Salman, M.; Yadav, G. C.; Sharma, S.; Kapkoti, G. S.; Chugh, A.; Gupta, J. B.; Anand, N. WO 2,003,084,928, 2003.
18. Salman, M.; Sharma, S.; Yadav, G. C.; Kapkoti, G. S.; Mishra, A.; Gupta, P.; Anand, N.; Chugh, A. Nanda, K. WO 2,005,118,537, 2005.
19. Kuo, G. H.; Prouty, C.; Murray, W. V.; Pulito, V.; Jolliffe, L.; Cheung, P.; Varga, S.; Evangelisto, M.; Wang, J. *J. Med. Chem.* **2000**, *43*, 2183.
20. Kuo, G. H.; Prouty, C.; Murray, W. V.; Shah, R. D. *J. Heterocycl. Chem.* **2001**, *38*, 1003.
21. Xu, F.; Chen, H.; He, X. L.; Xu, J. Y.; Xu, B. B.; Huang, B. Y.; Liang, X.; Yuan, M. *Molecules* **2014**, *19*, 12699.
22. Li, M.; Fang, H.; Du, L.; Xia, L.; Wang, B. *J. Mol. Model.* **2008**, 14957.
23. SOSUI programweb site: http://bp.nuap.nagoya-u.ac.jp/sosui/sosui_sumit.html.
24. NCBI BLAST web site: http://blast.ncbi.nlm.nih.gov/Blast.cgi.
25. Cherezov, V.; Rosenbaum, D. M.; Hanson, M. A.; Rasmussen, S. G.; Thian, F. S.; Kobilka, T. S.; Choi, H. J.; Kuhn, P.; Weis, W. I.; Kobilka, B. K.; Stevens, R. C. *Science* **2007**, *318*, 1258.
26. Wang, Q.; Mach, R. H.; Luedtke, R. R.; Reichert, D. E. *J. Chem. Inf. Model.* **2010**, *50*, 1970.